

Macroscopic effects of the spectral structure in turbulent flows

Tuan Tran¹, Pinaki Chakraborty², Nicholas Guttenberg³, Alisia Prescott⁴, Hamid Kellay⁵, Walter Goldberg⁴, Nigel Goldenfeld^{3*} and Gustavo Gioia^{1*}

¹*Department of Mechanical Science and Engineering, University of Illinois, Urbana, IL 61801, USA*

²*Department of Geology, University of Illinois, Urbana, IL 61801, USA*

³*Department of Physics, University of Illinois, Urbana, IL 61801, USA*

⁴*Department of Physics and Astronomy, University of Pittsburgh, Pittsburgh, PA 15260, USA*

⁵*Centre de Physique Moléculaire Optique et Hertzienne, Université Bordeaux I, 33405 Talence, France*

* *These authors contributed equally to this work*

Two aspects of turbulent flows¹⁻⁴ have been the subject of extensive, split research efforts: macroscopic properties, such as the frictional drag⁵ experienced by a flow past a wall, and the turbulent spectrum.^{1,6,7} The turbulent spectrum may be said to represent the fabric of a turbulent state; in practice it is a power law of exponent α (the “spectral exponent”) that gives the revolving velocity of a turbulent fluctuation (or “eddy”) of size s as a function of s .¹ The link, if any, between macroscopic properties and the turbulent spectrum remains missing. Might it be found by contrasting the frictional drag in flows with differing types of spectra? Here we perform unprecedented measurements of the frictional drag in soap-film flows,⁸ where the spectral exponent $\alpha = 3$,^{9,10} and compare the results with the frictional drag in pipe flows,⁵ where the spectral exponent $\alpha = 5/3$.^{11,12} For moderate values of the Reynolds number Re (a measure of the strength of the turbulence), we find that in soap-film flows the frictional drag scales as $Re^{-1/2}$, whereas in pipe flows the frictional drag scales¹³ as $Re^{-1/4}$. Each of these scalings may be predicted from the attendant value of α by using a new theory,^{14,15} in which the frictional drag is explicitly linked to the turbulent spectrum. Our work indicates that in turbulence, as in continuous phase transitions, macroscopic properties are governed by the spectral structure of the fluctuations.^{16,17}

Turbulent flows past a wall experience frictional drag, the macroscopic property of a flow that sets the cost of pumping oil through a pipeline, the draining capacity of a river in flood, and other quantities of engineering interest^{2,3,5,18,19}. The frictional drag is defined as the dimensionless ratio $f = \tau/\rho U^2$, where τ is the shear stress or force per unit area that develops between the flow and the wall, ρ is the density of the fluid, and U is the mean velocity of the flow. Already in XVIII Century France, f was the subject of large-scale experiments performed in connection with the design of a waterworks for the city of Paris.^{20,21} Modern experiments with pipes have shown that f depends on the Reynolds number $Re = Ud/\nu$, where d is the diameter of the pipe and ν is the

kinematic viscosity of the fluid. For pipe flows of moderate turbulent strength (Re up to 98,000) the experimental results are well described (within 1.4% error¹³) by the Blasius empirical scaling, $f \propto \text{Re}^{-1/4}$. (Throughout this paper, the symbol “ \propto ” may be changed to the symbol “ $=$ ” by introducing a dimensionless proportionality factor, e.g., $f = C \text{Re}^{-1/4}$.) A celebrated theory^{3,5} of the frictional drag was formulated eighty years ago by Ludwig Prandtl, the founder of turbulent hydraulics, and numerous variants^{5,13,22} and alternatives^{23,24} of Prandtl’s theory have since been proposed. Although Prandtl’s theory and its variants and alternatives yield disparate mathematical expressions for f as a function of Re, for moderate values of Re they all give predictions in good numerical accord with the Blasius empirical scaling. Yet these theories have been predicated on dimensional analysis and similarity assumptions, without reference to the spectral structure of the turbulent fluctuations. As a result, these theories cannot be used to reveal the missing link between the frictional drag and the turbulent spectrum.

The turbulent spectrum is a function of the wavenumber k , $E(k)$, whose physical significance may be grasped from the expression $u_s \propto (\int_{1/s}^{\infty} E(k) dk)^{1/2}$, which gives the revolving velocity u_s of a turbulent eddy of size s in the flow. In general, we can write¹⁵ $E(k) \propto U^2 L^{(1-\alpha)} k^{-\alpha}$, and therefore

$$u_s \propto U (s/L)^{(\alpha-1)/2}, \quad (1)$$

where α is the spectral exponent, U is the mean velocity of the flow, and L is a characteristic length. A single type of spectrum is possible in three-dimensional (3D) flows: the “energy cascade,” for which $\alpha = 5/3$.^{12,25} Thus, e.g., in turbulent pipe flows the spectral exponent is $5/3$ and $L = d$, the diameter of the pipe. Two-dimensional (2D) turbulence (a type of turbulence that may be realized in a soap film) differs from 3D turbulence in a number of crucial respects, most notably in that in two dimensions there is no vortex stretching. As a result, a different type of spectrum is possible in 2D flows: the “enstrophy cascade,” for which $\alpha = 3$.^{9,10} Thus, e.g., in turbulent soap-film flows the spectral exponent is 3 and $L = w$, the width of the soap film.

To study soap-film flows we hang a soap film between two long, vertical, mutually parallel wires a few centimeters apart from one another (Fig. 1a). Driven by gravity, a steady vertical flow soon becomes established within the film. Then, the thickness h of the film is roughly uniform on any cross section of the film, typically $h \approx 10 \mu\text{m}$, much smaller than the width w and the length of the film (Fig. 1a). As a result, the velocity of the flow lies on the plane of the film, and the flow is 2D.

We make the flow turbulent by piercing the film with a comb, as indicated in Fig. 1a, so that the flow is stirred as it moves past the teeth of the comb. To visualize the flow, we cast monochromatic light on a face of a film and observe the interference fringes that form there. These fringes (Fig. 1b) reflect small changes in the local thickness of the film. (The thickness is constant along a fringe; it differs by one-half wavelength of the light, or a fraction of a μm , between any two successive fringes.) The small changes in thickness in turn reflect small changes in the absolute value of the instantaneous velocity of the flow.⁸ Thus Fig. 1b may be interpreted as a map of the

instantaneous spatial distribution of turbulent fluctuations downstream of the comb.

We compute the spectrum $E(k)$ at numerous points on the film from measurements performed with a Laser Doppler Velocimeter (LDV; see Methods). In Fig. 1c we show a few typical log-log plots of E vs. k . The slope of these plots represents the spectral exponent α ; in our experiments the slope is slightly larger than 3, consistent with prior experiments with soap-film flows^{8,26}, and close to the theoretical value of α for the enstrophy cascade ($\alpha = 3$).

By using the same Laser Doppler Velocimeter we measure the mean (time-averaged) velocity u at any point on the film (see Methods). Successive measurements of u along a cross section of the film gives the “mean velocity profile” $u(y)$ of that cross section. In Fig. 2a we show a few typical plots of $u(y)$ over the entire width of the film (i.e., from wire to wire, or for $0 \leq y \leq w$; see Fig. 1a). From a mean velocity profile we compute the mean velocity of the flow as $U = (1/w) \int_0^w u(y) dy$, and the Reynolds number as $Re = Uw/\nu$.

In Fig. 2b we show a few typical plots of $u(y)$ close to one of the wires, where the mean velocity profile is linear on a narrow (about 0.2 mm) viscous layer. From the slope G of the mean velocity profile in the viscous layer, we compute the shear stress between the flow and the wire as $\tau = \rho\nu G$, and the frictional drag as $f = \tau/\rho U^2 = \nu G/U^2$. In Fig. 3 we show a log-log plot of f vs. Re . The plot consists of five sets of data points from numerous turbulent soap-film flows; four sets were taken at Pittsburgh, and one at Bordeaux in an independent experimental setup. The cloud of data points is consistent with the scaling, $f \propto Re^{-1/2}$, and inconsistent with the Blasius empirical scaling, $f \propto Re^{-1/4}$, which is known to prevail in turbulent pipe flows.

Our experimental results may be explained using a recently proposed theory of the frictional drag.^{14,15} In this new theory, the frictional drag is produced by turbulent eddies that transfer momentum between the wall or wire (where the fluid carries a negligible momentum per unit mass) and the turbulent flow (where the fluid carries a sizable momentum per unit mass). The theory is generally applicable to flows that move past rough walls, but for the special case in which the wall is smooth (as in our experiments), the theory predicts that $f \propto u_\eta/U$,^{14,15,17,27–29} where η is the size of the smallest eddies in the flow and u_η is the revolving velocity of those eddies. Note that in this scaling for f , u_η provides a connection to the turbulent spectrum, as shown next.

To a generic eddy of size s we ascribe an eddy Reynolds number $Re_s = u_s s/\nu$, where u_s is the revolving velocity of the eddy. The Reynolds number of the smallest eddies in the flow is of order 1 (because these eddies are viscous^{1,12}), and we can write $Re_\eta = u_\eta \eta/\nu \approx 1$, or $u_\eta \propto \nu/\eta$. A second expression for u_η may be obtained from the spectrum by setting $s = \eta$ in (1); if we combine these two expressions so as to eliminate η , we can write $u_\eta \propto U Re^{(1-\alpha)/(1+\alpha)}$, where we have used the definition $Re = UL/\nu$. As $f \propto u_\eta/U$, it follows that

$$f \propto Re^{(1-\alpha)/(1+\alpha)}, \quad (2)$$

and the functional dependence of the frictional drag on the Reynolds number is set by the spectral

exponent α . For pipe flows $\alpha = 5/3$, and (2) yields the prediction¹⁴ $f \propto \text{Re}^{-1/4}$, consistent with the Blasius scaling. In contrast, for soap-film flows $\alpha = 3$, and (2) yields the prediction¹⁵ $f \propto \text{Re}^{-1/2}$, consistent with our experimental results (Fig. 3).

From our experiments with two-dimensional soap-film flows we infer that the long-standing and widely-accepted theory⁵ of the frictional drag between a turbulent flow and a wall is incomplete. This classical theory does not take into account the structure of the turbulent fluctuations, and cannot distinguish between two-dimensional and three-dimensional turbulent flows. Our data on soap-film flows, as well as the available data on pipe flows, are, however, consistent with the predictions of a recently proposed theory of the frictional drag.^{14,15} This new theory perforce relates the frictional drag to the turbulent spectrum, and is sensitive to the dimensionality of the flow via the dependence of the turbulent spectrum on the dimensionality. Our findings lead us to conclude that the macroscopic properties of both three-dimensional and two-dimensional turbulent flows are linked to the turbulent fluctuations, in a manner analogous to the way in which order-parameter fluctuations are linked to the macroscopic properties of thermodynamic systems close to a critical point.^{16,17} In addition, our findings serve to underscore the value of using two-dimensional soap-film flows to test and extend our understanding of turbulent phenomena.

Methods

We measure the vertical component $u(t)$ of the instantaneous velocity at a point on the film using a Laser Doppler Velocimeter with a sampling rate of 5 kHz. By performing measurements over a time period of about 10 s, we collect a time series $u(t_i)$. From the time series we compute the local mean velocity u as the time average of $u(t_i)$, $u = \langle u(t_i) \rangle$. From the same time series $u(t_i)$ we compute the local turbulent spectrum (more precisely, the longitudinal turbulent spectrum). To that end, we invoke Taylor’s frozen-turbulence hypothesis⁶ to perform a space-for-time substitution $t \rightarrow x/u$ on the time series $(u(t_i) - u)$ to obtain a space series $v(x_i) = (u(x_i/u) - u)$, where $x_i = ut_i$. (The frozen-turbulence hypothesis is justified because in all our experiments the root mean square of the velocity fluctuations is less than 20% of u .³⁰) The spectrum $E(k)$ is the square of the magnitude of the discrete Fourier transform of $v(x_i)$.

1. Frisch, U. *Turbulence: The Legacy of A.N. Kolmogorov* (Cambridge University Press, Cambridge, UK, 1995).
2. Sreenivasan, K. R. Fluid turbulence. *Rev. Mod. Phys.* **71**, S383–S395 (1999).
3. Pope, S. *Turbulent Flows* (Cambridge University Press, Cambridge, UK, 2000).
4. Hof, B., Westerweel, J., Schneider, T. & Eckhardt, B. Finite lifetime of turbulence in shear flows. *Nature* **443**, 59–62 (2006).
5. Schlichting, H. & Gersten, K. *Boundary-Layer Theory* (Springer, New York, USA, 2000).

6. Taylor, G. The spectrum of turbulence. *Proceedings of the Royal Society of London. Series A, Mathematical and Physical Sciences* 476–490 (1938).
7. Sreenivasan, K. R. The phenomenology of small-scale turbulence. *Annu. Rev. Fluid Mech.* **29**, 435–472 (1997).
8. Kellay, H. & Goldburg, W. I. Two-dimensional turbulence: a review of some recent experiments. *Rep. Prog. Phys.* **65**, 845–894 (2002).
9. Kraichnan, R. H. Inertial ranges in two-dimensional turbulence. *The Physics of Fluids* **10**, 1417–1423 (1967).
10. Batchelor, G. *The Theory of Homogeneous Turbulence* (Cambridge University Press, Cambridge, UK, 1953).
11. Richardson, L. F. Atmospheric diffusion shown on a distance–neighbour graph. *Proc. Roy. Soc. London A* **110**, 709–737 (1926).
12. Kolmogorov, A. N. Local structure of turbulence in incompressible fluid at a very high reynolds number. *Dokl. Akad. Nauk. SSSR* **30**, 299–302 (1941). [English translation in Proc. R. Soc. London Ser. A 434 (1991)].
13. Mckeon, B. J., Zagarola, M. V. & Smits, A. J. A new friction factor relationship for fully developed pipe flow. *Journal of Fluid Mechanics* **538**, 429–443 (2005).
14. Gioia, G. & Chakraborty, P. Turbulent friction in rough pipes and the energy spectrum of the phenomenological theory. *Phys. Rev. Lett* **96**, 044502 (2006).
15. Guttenberg, N. & Goldenfeld, N. Friction factor of two-dimensional rough-boundary turbulent soap film flows. *Physical Review E (Statistical, Nonlinear, and Soft Matter Physics)* **79**, 065306 (2009).
16. Goldenfeld, N. Roughness-Induced Critical Phenomena in a Turbulent Flow. *Phys. Rev. Lett.* **96**, 044503 (2006).
17. Mehrafarin, M. & Pourtolami, N. Intermittency and rough-pipe turbulence. *Phys. Rev. E* **77**, 055304 (2008).
18. Nikuradze, J. Stromungsgesetze in rauhen Rohren. *VDI Forschungsheft* **361** (1933). [English translation available as National Advisory Committee for Aeronautics, Tech. Memo. 1292 (1950). Online at: <http://hdl.handle.net/2060/19930093938>].
19. Jimenez, J. Turbulent flows over rough walls. *Annual Review of Fluid Mechanics* **36**, 173–196 (2004).
20. Chézy, A. Memoire sur la vitesse de l’eau conduit dans une rigole donne. In *Dossier 847 (MS 1915)* (Ecole des Ponts et Chaussees, 1775). [English translation in Journal, Association of Engineering Societies, vol 18, 363–368, 1897].

21. Dooge, J. C. I. The manning formula in context. In Yen, B. C. (ed.) *Channel flow resistance: centennial of Manning's formula*, 136–185 (Water Resources Publications, Littleton, Colorado, 1992).
22. Allen, J. J., Shockling, M. A., Kunkel, G. J. & Smits, A. J. Turbulent flow in smooth and rough pipes. *Phil. Trans. Roy. Soc. A* **365**, 699–714 (2007).
23. Barenblatt, G. Scaling laws for fully developed turbulent shear flows. Part 1. Basic hypotheses and analysis. *Journal of Fluid Mechanics* **248**, 513–520 (1993).
24. Barenblatt, G. & Chorin, A. A mathematical model for the scaling of turbulence. *Proceedings of the National Academy of Sciences* **101**, 15023–15026 (2004).
25. Obukhov, A. M. Energy distribution in the spectrum of turbulent flow. *Dokl. Akad. Nauk. SSSR* **32**, 22–24 (1941).
26. Kellay, H., Wu, X. & Goldburg, W. Experiments with Turbulent Soap Films. *Physical Review Letters* **74**, 3975–3978 (1995).
27. Gioia, G. & Bombardelli, F. A. Scaling and similarity in rough channel flows. *Phys. Rev. Lett.* **88**, 014501 (2002).
28. Gioia, G., Chakraborty, P. & Bombardelli, F. A. Rough-pipe flows and the existence of fully developed turbulence. *Phys. Fluids* **18**, 038107 (2006).
29. Calzetta, E. Friction factor for turbulent flow in rough pipes from Heisenberg's closure hypothesis. *Physical Review E* **79**, 56311 (2009).
30. Belmonte, A., Martin, B. & Goldburg, W. Experimental study of Taylor's hypothesis in a turbulent soap film. *Physics of Fluids* **12**, 835–845 (2000).

Author Information Reprints and permissions information is available at npg.nature.com/reprints and permissions. The authors declare that they have no competing financial interests.

Acknowledgements We thank discussions with J. M. Larkin. This work was funded by the US National Science Foundation through NSF/DMR grant 06-04477 and NSF/DMR grant 06-04435 (W. Fuller–Mora, Programme Director). T. Tuan acknowledges support from the Vietnam Education Foundation.

Author Contributions Experiments were performed primarily in Pittsburgh by T. Tuan, and in Bordeaux by H. Kellay. Analysis of data was carried out by all authors. Research was designed by G. Gioia, N. Goldenfeld, and W. Goldburg. G. Gioia wrote the paper with assistance from N. Goldenfeld and P. Chakraborty (who also wrote the Supplementary Information).

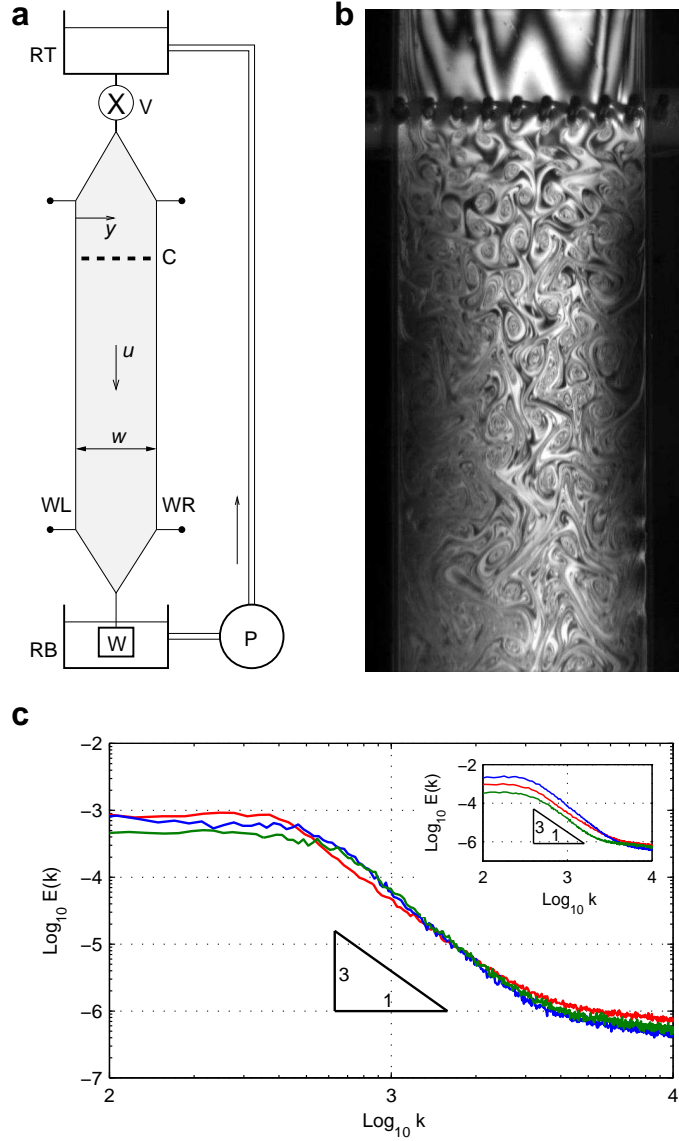


Figure 1: Experimental setup used to study steady, gravity-driven, 2D soap-film flows. **(a)** Wires WL and WR are thin nylon wires (diameter = 0.5 mm) kept taut by weight W. The film hangs from the wires; its width increases from 0 to w over an expansion section, then remains constant and equal to w over a section of length ≈ 1 m. Reservoir RT contains a soapy solution (2.5% Dawn Nonultra in water; $\nu = 0.01 \text{ cm}^2/\text{s}$), which flows through valve V and into the film. After flowing through the film, the soapy solution drains into reservoir RB and returns to reservoir RT via pump P. Turbulence is generated by comb C of tooth diameter ≈ 0.5 mm and tooth spacing ≈ 3 mm. We perform all measurements at a distance of at least 10 cm downstream of the comb. Axis y ($0 \leq y \leq w$) has its origin at wire WL, as indicated. **(b)** Interference fringes in yellow light (wavelength = $0.6 \mu\text{m}$) make it possible to visualize the generation of 2D turbulence from the comb. **(c)** Typical log-log plots of the spectrum $E(k)$, from LDV measurements performed on points of the film close to one of the wires and (inset) along the centerline of the flow

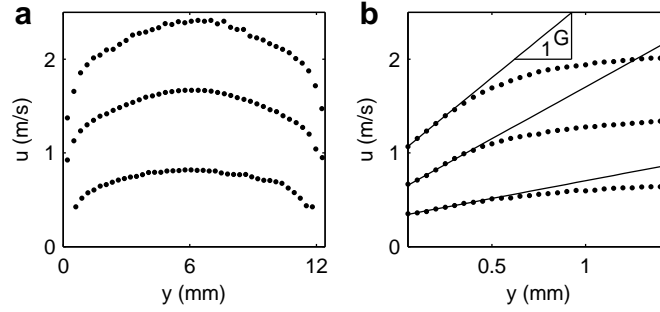


Figure 2: The mean velocity profile $u(y)$ in turbulent soap-film flows, from LDV measurements. **(a)** Typical plots of $u(y)$ in a film of width $w = 12$ mm. **(b)** Typical plots of $u(y)$ close to one of the wires, in the viscous layer where $du(y)/dy = G$ and the thickness of the film is uniform and $\approx 10 \mu\text{m}$ (Supplementary Information). The velocity profiles correspond to $\text{Re} = 7893, 17648, 25912$. Points on the film closer than $\approx 20 \mu\text{m}$ (the diameter of the beam of the LDV) from the edge of the wire cannot be probed with the LDV; thus the first data point, which we position at $y = 0$, is at a distance of $\approx 20 \mu\text{m}$ from the edge of the wire. The apparent slip velocity is likely to represent 3D and surface-tension effects associated with the complex flow at the contact between the film and the wire.

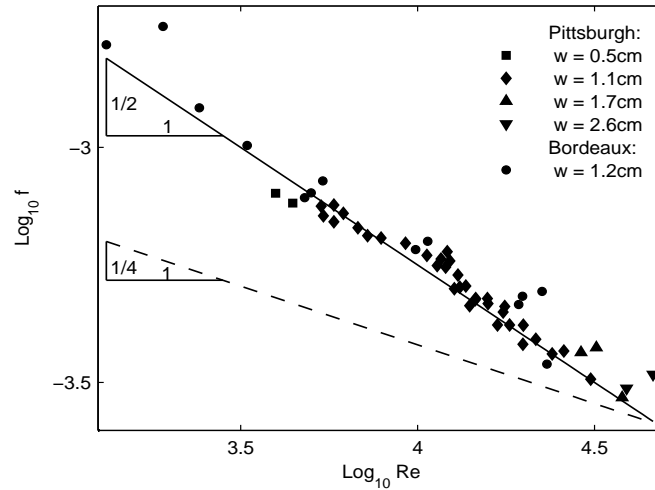


Figure 3: Log-log plot of the frictional drag vs. the Reynolds number in 2D turbulent soap-film flows of Reynolds number $1300 \leq \text{Re} \leq 25000$, from independent experiments performed in Pittsburgh and Bordeaux. The cloud of data points may be represented as a straight line of slope $1/2$, consistent with the scaling $f \propto \text{Re}^{-1/2}$. The straight dashed line of slope $1/4$ corresponds to the Blasius empirical scaling, $f \propto \text{Re}^{-1/4}$.